Polymer Vol. 39 No. 26, pp. 6685–6696, 1998

0032-3861/98/$ - see front matter

PII: S0032-3861(98)00097-4

polymer papers

Small angle neutron scattering from ionomer gels

A. M. Young[a,*], C. Brigault[a], R. Heenan[b], J. S. Higgins[c] and D. G. Peiffer[d]
[a]*Chemistry Department, Brunel University, Uxbridge, Middlesex UB8 3PH, UK*
[b]*Rutherford Appleton Laboratory, Didcot, Oxford OX11 OQX, UK*
[c]*Chemical Engineering Department, Imperial College, London SW7 2AZ, UK*
[d]*Exxon Research and Engineering Company, Route 22 East, Clinton Township, Annandale, NJ 08801, USA*
(Received 25 September 1997; revised 4 December 1997; accepted 8 January 1998)

Small angle neutron scattering intensities for sols and gels of the physically associating ionomer 1.39 mol% sodium sulphonated polystyrene with molecular weight 10^5 g/mole in xylene have been obtained over a broad wavevector (q) and concentration range. In the low q and concentration range the scattering behaviour of this ionomer/solvent system can quite readily be interpreted using the open association aggregation model. In more concentrated solutions and at higher q, however, interpretation of the scattering behaviour for polymers associating via an open association mechanism (OAM) is more difficult, particularly if, as in this investigation, the single chains and aggregates have varying densities and fractal parameters. In this study various methods have been developed to interpret the low and high q scattering from systems whose extent of aggregation can be modelled using the OAM. Using these methods it has been possible to confirm that the open association model can be used to interpret the extent of aggregation of the above ionomer in xylene even after the solutions appear to be gelled. Single ionomer chains within both the dilute solutions and gels were found via modelling to have a radius of gyration of 60 Å, which compares with dimensions of 25 Å and 93 Å calculated for a solid sphere of polystyrene or an unperturbed polystyrene Gaussian coil, respectively. The aggregates, however, all had radii of gyration comparable with what would be expected for polystyrene of the aggregate molecular weight in an unperturbed state. These results suggest that gelation of ionomer solutions at particular concentration thresholds is not due to an abrupt change in the aggregate structures at some critical concentration but occurs as a result of interactions between the very large aggregates that the OAM predicts should gradually form as the ionomer concentration increases.

(Keywords: ionomer; aggregation; gelation)

INTRODUCTION

The addition of a low level of ionic groups to a non-polar polymer to produce an ionomer can have very large effects on the solution properties of the polymer. In non-polar solvents, for example, the dilute solution viscosity of sulphonated polystyrene ionomers generally decreases to a minimum value (at a critical insolubility charge level dependent upon the solvent dielectric constant), as the number of ionic groups on the polymer is raised. In the semi-dilute regime, however, solutions of ionomers with close to the critical charge level can gel[1–3]. Applications for ionomers in non-polar solvents arising from their theological properties include viscosity index improvers in automotive lubricants, viscosifiers and stabilizers in drilling fluids and gels for poreblocking in oil wells[4,5]. A number of authors have attempted to characterize the structure of gels using both light and small angle neutron scattering techniques. Physically cross-linked gels that have recently been investigated include gelatin in water[6,7], syndiotactic polystyrene in chloroform[8] and polyvinyl alcohol in water/dimethyl sulphoxide mixtures[9]. In many of these studies the intensity of scattering at low angles shows a sharp upturn, indicating large-scale inhomogeneities due to polymer aggregation within the gels. Aggregates can also often still be detected when the gels are diluted to form solutions. A quantitative method of characterizing these inhomogeneities is made difficult, however, because their size can be concentration-, sample preparation technique- and time-dependent. One aim of this paper is to describe a new method of interpreting the scattering from gels using well aged and characterized ionomer gels as a model system.

In dilute solutions ionomers can form both intra- and intermolecular ion pair associations making interpretation of even the very dilute solution viscosities complex. A combination of light[10] and small angle neutron scattering (SANS)[11,12] studies has shown that the intramolecular associations can lead to the polymer collapsing into a compact sphere that occupies relatively little volume. As the polymer concentration is increased (within the dilute concentration regime), intermolecular ion pair associations form at the expense of intramolecular ones and single chain expansion combined with aggregation can be observed[12,13]. The dilute solution aggregation behaviours of some monodisperse (molecular weight of 10^5 g/mol) sodium sulphonated polystyrene ionomers (SPS) in xylene have been investigated in detail using these scattering methods. In this non-polar solvent the ionomer becomes insoluble at charge levels greater than 1.65 mol%. Below 0.62 mol% sulphonation no ion pair associations (either intra or inter) appear to occur[14]. At 0.95 mol% sulphonation, however, compact single chains in equilibrium with compact

* To whom correspondence should be addressed

aggregates consisting of three chains only are observed in the dilute solutions[12]. This kind of limited size aggregation can be classified as a closed association process[15]. When the sulphonation level exceeds 1.25 mol%, however, a change in the aggregation behaviour occurs, with single collapsed chains found to be in equilibrium with aggregates of all sizes[11]. As the polymer concentration is raised within the dilute solution regime the average size of the aggregates increases. In this latter case the open association model[15] explains the concentration dependence of the aggregation process.

Recent work has shown that the viscosity of dilute ionomer solutions is dependent primarily on the total volumes occupied by the aggregates and single chains in all the above ionomer systems[14]. When concentrations of these ionomer solutions exceed 0.5 g/dl the viscosities are much larger than predicted from the total volumes occupied by the polymer chains indicating that interaggregate interactions become important in determining rheological effects above this concentration[14]. This is most evident with solutions of the SPS in xylene with sulphonation levels between 1.25 and 1.65 mol% since these gel when the polymer concentration exceeds 2 g/dl. Recent work suggests that the observation of an open association process in dilute solution may be a common feature for ionomer solutions that gel on increasing the concentration into the semi-dilute regime[14]. It is not known, however, whether the model can also explain the state of aggregation of the chains within well aged ionomer gels. No studies have been reported that successfully manage to quantitatively explain the variation in ionomer chain aggregation with concentration within a gel as would be demonstrated by the ability to fit an association model to gel scattering data. Therefore, it is not known whether the gelation arises through entanglements between the aggregates as they begin to overlap at 2 g/dl or if it is due to a sudden change in the structure of the aggregates at this concentration.

SANS studies on gelling telechelic (ionic groups at chain ends only) carboxylated polystyrene ionomer solutions have been carried out by two groups[16,17]. Difficulties arise in a full interpretation of the results, however, due to the combination of changing aggregation with concentration and interparticle scattering (which is a much more dominant feature in semi-dilute solutions). In both the reports on telechelic gel scattering a much broader range of wavevector (q) was used when compared with all the studies described above on random SPS ionomers. The use of much higher q results, in principle, should aid in the interpretation of scattering since interparticle effects usually decrease relative to intraparticle scattering as q increases. Further data interpretation difficulties arise, however, in that the shape of scattering objects affects high q scattering, whereas this can be ignored at low q. The two groups already mentioned, although investigating almost identical (at least chemically) telechelic ionomer solutions, unfortunately arrive at very different conclusions about the effect of molecular weight on the association process and in particular the variations in average aggregate dimensions with concentration. This could be due either to the solutions being at different stages of ageing and/or to the different methods of data interpretation used in each case. In order to fit the intensities of scattering versus q, different models developed primarily for non-associating monodisperse polymers were used in the two studies.

If the closed association model can describe the extent of aggregation of a polymer then the use of methods developed for monodisperse systems to interpret scattering data is often reasonable, since at low concentrations only single chains are present but at high concentrations 'monodisperse' aggregates dominate the scattering behaviour. For a polymer aggregating via the open association model, however, the following paper will show that interpretation of scattering data can be much more complex. In the present study the variation in scattering versus q for systems aggregating via such a process will be calculated for a range of different model cases. These models shall be compared with some new data for random SPS ionomer gels obtained over a broad q range.

THEORY

In the following section theories often used to interpret the scattering from polydisperse polymer solutions will first be summarized. The equations given will then be used and extended to provide general equations for the scattering from polymers associating via an open association process. The applicability of the equations derived to polystyrene and ionomer solution scattering data will be discussed in the Results section.

Non-aggregating polymers[18–23]

The Zimm expression interprets the normalized coherent scattering from a non-aggregating polydisperse polymer solution as a function of the scattering vector, q, as

$$\kappa c/I(q) = 1/\sum [w_i M_i S_i(q)] + [2A_2 c + 3A_3 c^2 + \ldots] \quad (1)$$

where $I(q)$ is the normalized intensity and c is the total polymer concentration in units of weight per unit volume. The constant κ is given by

$$\kappa = (N_a/m^2)(a_p - a_s\{V_m/V_s\})^2 \quad (2)$$

N_a is Avogadro's number and m the polymer monomer molecular weight. a_p and a_s are the scattering length densities of the polymer and solvent. V_m and V_s are the molar volumes of the monomer unit and solvent. For polystyrene (PS) and the ionomer (SPS) in xylene the constant κ can be taken as approximately equal (given the low levels of ionic groups in the SPS samples used) and is calculated using measured densities of polystyrene/xylene solutions to be 2.66×10^{-3} mol g^2 cm^2 at 25°C.

The second term in square brackets in equation (1) arises from interparticle scattering effects. The virial coefficients, A_2 and A_3, account for the non-ideality of the system and can be related to the excess Gibbs free energy of the solvent on dissolution of the polymer[15]. Previous results for polystyrene in toluene indicate that as a first approximation the virial coefficients can be assumed to be constants that are independent of q[22]. The first term in square brackets is an intraparticle scattering term, w_i is the weight fraction of species of molecular weight M_i. $S_i(q)$ is a particle scattering factor which for solid spheres is given by

$$S_i(q) = [(3/\mu_i^3)\{\sin\mu_i - \mu_i\cos\mu_i\}]^2 \quad (3)$$

where $\mu_i = qR_i$. R_i is the radius of the sphere, which is related to its radius of gyration Rg_i by

$$R_i = (5/3)^{0.5} Rg_i$$

For Gaussian coils, the Debye expression gives

$$S_i(q) = [(2/u_i^4)(\exp\{-u_i^2\} - 1 + u_i^2)] \quad (4)$$

with $u_i = qRg_i$. This expression has also been shown to be

valid for slightly expanded polymers in good solvents for values of u up to approximately 4. Alternatively at $u_i \ll 1$ using the Guinier approximation $S_i(q)$ becomes independent of the particle shape and

$$S_i(q)_{q\to 0} \approx 1 - \exp(-u_i^2/3)$$

If the exponential term is rewritten as a truncated series then

$$S_i(q)_{q\to 0} \approx 1 - u_i^2/3 \approx 1/(1 + u_i^2/3) \quad (5)$$

It can be shown by combining equation (1) and equation (5) that in the low q range

$$\kappa c/I(q)_{q\to 0} = [(1/\langle M\rangle_w)(1 + u_z^2)/3)] + [2\mathrm{A}_2 c + 3\mathrm{A}_3 c^2 + \ldots] \quad (6)$$

where ${u_z}^2 = q^2\langle Rg^2\rangle_z$. The weight average molecular weight is given by

$$\langle M\rangle_w = \sum w_i M_i \quad (7)$$

and the so-called z-average radius of gyration squared by

$$\langle Rg^2\rangle_z = \sum w_i M_i Rg_i^2/(\sum w_i M_i) \quad (8)$$

To obtain equation (6), it is assumed that equation (5) is valid for all the species present. The max q used should therefore strictly be smaller than the inverse radius of gyration of the largest molecule. In many cases, however, this restriction can be relaxed without large errors being incurred (for an example see later). If the virial terms are not negligible then apparent molecular weights (M_{app}) and radii of gyration (Rg_{app}) are obtained from Zimm plots of $1/I$ versus q^2. These are defined as

$$1/M_{\mathrm{app}} = \kappa c/I(0) = 1/ < M >_w + 2\mathrm{A}_2 c + 3\mathrm{A}_3 c^2 + \ldots \quad (9)$$

and

$$Rg^2_{\mathrm{app}} = 3I(0)\{d[1/I(q)]/dq^2\} = < Rg^2 >_z M_{\mathrm{app}}/ < M >_w \quad (10)$$

For this work an apparent second virial coefficient defined as

$$\mathrm{A}_{2,\mathrm{app}} = (1/M_{\mathrm{app}} - 1/ < M >_w)/(2c) = \mathrm{A}_2 + (3/2)\mathrm{A}_3 c + \ldots \quad (11)$$

will also be used.

In many cases[21] at sufficiently large u_i (typically greater than about 3) it can be shown that for fractal objects

$$S_i(q)_{q\to\infty} \approx \mathrm{A} u_i^{-D} \quad (12)$$

where D is the fractal dimension and A is a constant equal to 2 for Gaussian chains. D is the exponent in the relation between molecular dimensions and molecular weight

$$Rg_i = \mathrm{C} M_i^{1/D} \quad (13)$$

D is 3 for a solid object, 2 for a planar one and a Gaussian coil and 1 for a linear molecule. It can be obtained from the gradient of log I versus log q or from Kratky plots of $I(q)q^D$ against q or q^2. If a Kratky plot has a horizontal asymptote then the value of the exponent D is confirmed. C is a constant.

To fit the full q range simultaneously for a polymer solution equations such as equation (1) and equation (4) need to be combined. For a monodisperse non-aggregating Gaussian polymer of molecular weight M_1 and radius of gyration R_{g1} from equations (1) and (4) the predicted shape of $\kappa \mathrm{c} \mathrm{M}_1/I(q)$ versus u_1 is expected to be dependent upon the interparticle scattering term only. If $2\mathrm{A}_{2,\mathrm{app}} M_1 c$ is independent of q then general curves of $\kappa cM/I(q)$ versus u can be given (see *Figure 1*). Many of the programs generally available to fit the Debye expression to scattering data over a broad q range allow M_1, Rg_1 and a constant background value as the only fitting parameters. The virial term, however, from *Figure 1* clearly alters the shape of the scattering curves. It should therefore be taken into account for non-dilute monodisperse polymer solutions when fitting the Debye expression over a broad q range.

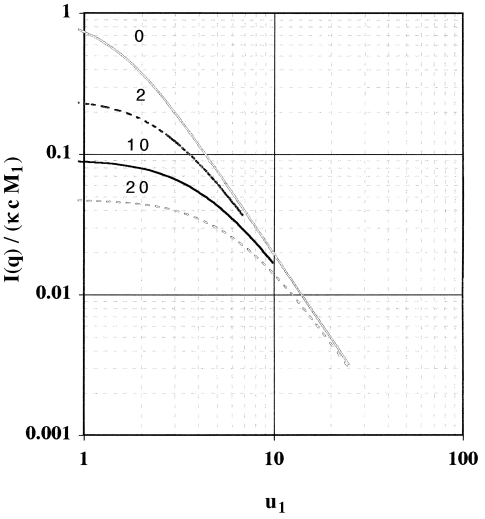

Figure 1 Calculated scattering for a monodisperse Gaussian polymer with interparticle interactions included (equation (1) with equation (4)). Values for $2\mathrm{A}_2 M_1 c$ for each curve on given on the figure

Aggregating polymers

Recent work[11,12] on dilute ionomer solutions suggest that equation (1) is also valid for associating polymers provided i refers to all the scattering objects (i.e. both the single chains and aggregates) in the solution. For an associating polymer solution equation (1) with equation (11) then becomes

$$\kappa c M_1/I(q) = 1/[\{w_1 S_1(q) + \sum (n w_n S_n(q))\}] + [2\mathrm{A}_{2,\mathrm{app}} M_1 c] \quad (14)$$

The subscripts 1 and n indicate values for single chains or aggregates consisting of n chains, respectively.

Low q scattering. In the low q range using equations (5) and (14) the general expression

$$\kappa c M_1/I(q)_{q\to 0} \approx [1/x(1 + u_z^2/3)] + [2\mathrm{A}_{2,\mathrm{app}} M_1 c] \quad (15)$$

is obtained. The ratio

$$x = \langle M\rangle_w/M_1 \quad (16)$$

The weight average molecular weight of all the single chains and aggregates [$\langle M\rangle_w$ defined as in equation (7)] for aggregating polymers varies with polymer concentration. This is also true of the z-average radius of gyration in the term ${u_z}^2 (= q^2\langle Rg^2\rangle_z)$. A model is therefore first required to explain the concentration dependence of x.

In the open association aggregation model (OAM) single chains are assumed to be in equilibrium with aggregates of all sizes, i.e.

$$P_1 + P_1 \Leftrightarrow P_2 \quad K_2$$

$$P_1 + P_2 \Leftrightarrow P_3 \quad K_3$$

$$P_1 + P_n \Leftrightarrow P_{n+1} \quad K_{n+1}$$

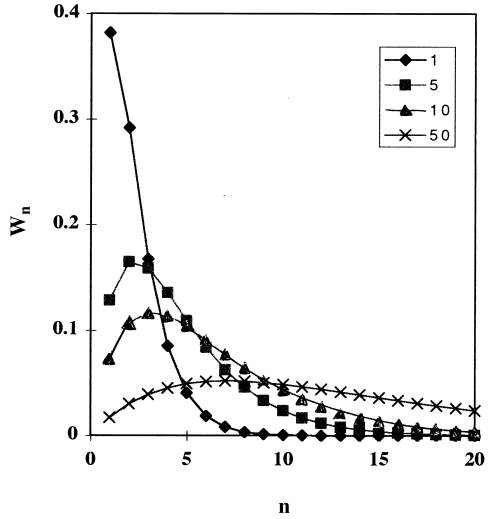

Figure 2 Calculated weight fractions of aggregates, w_n, versus number of chains in the aggregate, n, for a system aggregating via the open association model at various values of Kc/M_1. Values of Kc/M_1 for each distribution are given in the figure

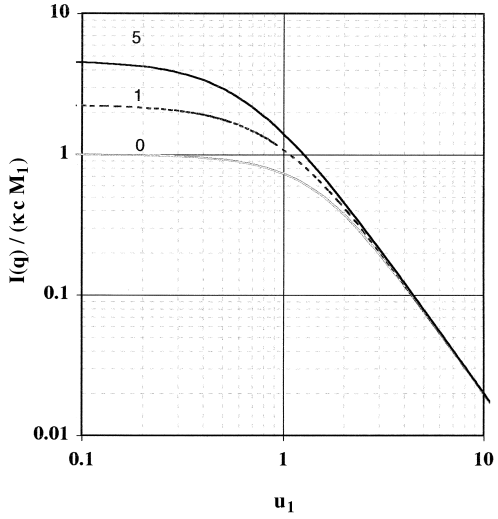

Figure 3 Calculated single chain molecular weight normalized scattering for a system aggregating via the open association model where all the scattering objects are assumed to be like Gaussian coils. Values for Kc/M_1 for each curve are given on the figure

where P_n is an aggregate consisting of n chains. If the equilibrium constants for each step are invariant with increases in the size of the aggregates then

$$K = K_2 = K_3 = [P_2]/[P_1]^2 \tag{17}$$

$[P_1]$ and $[P_2]$ are the molar concentrations of the single chains and two chain aggregates, respectively. In this case x becomes[15]

$$x = \langle M \rangle_w / M_1 = \{1 + (4Kc/M_1)\}^{0.5} \tag{18}$$

The weight fractions of single chains and aggregates of n chains at a particular Kc/M_1 value are also given by[15]

$$w_1 = (M_1/Kc)[(x-1)/(x+1)] \tag{19}$$

and

$$w_n = n(Kc/M_1)^{n-1} w_1^n \tag{20}$$

It should be noted from equations (18)–(20) that x, w_1 and w_n are all determined by the value of Kc/M_1 only. The distributions of single chains and aggregates at values of Kc/M_1 equal to 1, 5, 10 and 50 calculated using equations (18)–(20) are given in *Figure 2*. If for example K/M_1 is equal to 1 dl g^{-1} for a polymer whose aggregation behaviour is described by the OAM, then the four curves given in *Figure 2* give the weight fractions of all the various aggregates and single chains at 1, 5, 10 and 50 g dl^{-1}. For $Kc/M_1 < 1$ there are significant levels of single chains. At $Kc/M_1 > 10$ most of the polymer chains are predicted to be in aggregates, some of which are very large.

The z-average radius of gyration for the aggregating polymer from equation (8) will be

$$\langle Rg^2 \rangle_z = (w_1 Rg_1^2 + \sum n w_n Rg_n^2)/x \tag{21}$$

Rg_n is the total radius of gyration of an aggregate consisting of n chains. In order to fit the variation of the observed z-average radii of gyration with concentration to a theoretical model it will be assumed that the aggregates are fractal so that equation (13) is valid. If the single chains have the same values for C and D as the aggregates then from equation (13) their radius of gyration Rg_1 would equal $Rg_n/n^{1/D}$. Previous studies[11] suggest, however, that the single chains form more compact structures than the aggregates and therefore that such an assumption could be invalid. To aid interpretation of results in the following, two extra parameters k and $Rg_{1,h}$ defined by

$$Rg_{1,h} = Rg_n/n^{1/D} = CM_1^{1/D} \tag{22}$$

and

$$k = Rg_{1,h}/Rg_1 \tag{23}$$

shall be used. k gives a measure of the compactness of the single chains relative to the aggregates. $Rg_{1,h}$ is a hypothetical radius of gyration of a single chain that has the same fractal parameters as the aggregates. In the following $Rg_{1,h}$ and D (from which the radius of gyration of any aggregate consisting of n chains can be calculated) and k (or Rg_1) will be fitted constants.

Intermediate and high q scattering. In discussing high q scattering several different model cases shall be considered. The use of equations (22) and (23) enables, for systems aggregating via the OAM, general intraparticle scattering curves of $I(q)/\kappa cM_1$ against ku_1 ($u_1 = qRg_1$) dependent upon D, k, Kc/M_1 and the equations used for $S_i(q)$ only to be generated. Some of these are described below.

With $k = 1$. With $k = 1$ and equation (4) for Gaussian coils used to calculate $S_i(q)$ for all structures in the solution then if both the single chains and aggregates are fractal D is equal to 2. Then the concentration and single chain molecular weight normalized scattering intensity, $I(q)/\kappa cM_1$, when plotted against u_1 will for the OAM be dependent upon the magnitude of Kc/M_1 and any interparticle scattering effects only. The variation of normalized intraparticle intensity with u_1 in double logarithmic form calculated using equation (14) with equation (4) [for all $S_i(q)$], equations (18)–(20) (which define w_i) and equation (22) with equation (23) (as expressions for Rg_i) is given by *Figure 3*. At high q all the curves become independent of Kc/M_1 and have an asymptotic gradient of -2. When the plots in *Figure 3* are normalized by the weight average molecular weight and z-average radius of gyration they also all converge at $u_z < 1$ (see for example *Figure 4*). *Figure 4* indicates that if the Debye model for a non-aggregating polymer is fitted to the model curve with

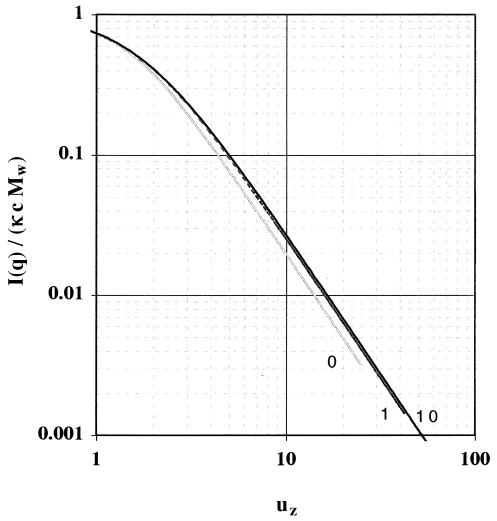

Figure 4 Calculated weight average molecular weight normalized scattering for a system aggregating via the open association model where all the scattering objects are assumed to be like Gaussian coils. Values for Kc/M_1 for each curve are given on the figure

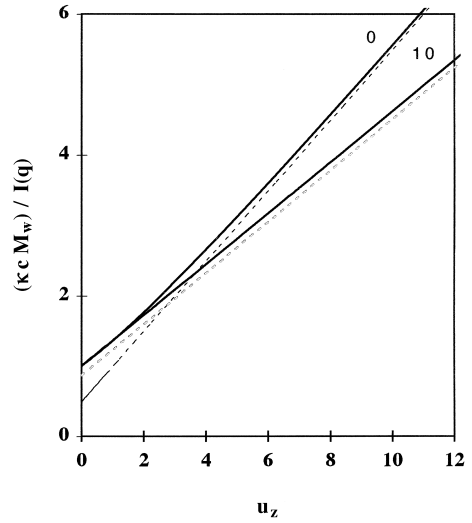

Figure 5 Calculated inverse weight average molecular weight normalized scattering for a system aggregating via the open association model where all the scattering objects are assumed to be like Gaussian coils. Values for Kc/M_1 for each curve are given on the figure. Dotted lines are extrapolated high q asymptotic behaviours calculated using equation (5)

$Kc/M_1 > 1$, Rg_z (equal to $\langle Rg_z \rangle_z^{0.5}$) could be obtained provided data at $u_z < 1$ only are used. If results in the range $1 < u_z < 10$ were used the model fitting would, however give values for Rg_z and $\langle M \rangle_w$ that are approximately 20 and 10% too small, respectively.

If the curves shown in *Figure 4* are plotted in the Zimm form (i.e. $[(\kappa cM_1)/I(q)]$ versus q^2) then it is observed that for $Kc/M_1 = 0$ (i.e. a monodisperse non-aggregating system) the Debye model deviates quite strongly from linearity after $u_z > 1$. With $Kc/M_1 = 10$, however, the Zimm plot remains practically linear over the whole q range (see *Figure 5*). To justify (in part) this observation mathematically, equation (4) can be simplified in an intermediate to high q range

$$S_i(q)_{u>1} \approx [2/u^2][1 - (1/u^2)] \tag{24}$$

Then combining equations (22)–(24) with equation (14) gives

$$[\kappa cM_1/I(q)]_{u1>1} = [u_1^2/2] + [1/2y] + [2A_{2,\text{app}}M_1c] \tag{25}$$

where

$$y = \langle M \rangle_n / M_1 \tag{26}$$

and $\langle M \rangle_n$ is the number average molecular weight. Rearranging equations given previously in Elias[15] it can be shown that for the open association model

$$2y = 1 + x \tag{27}$$

If $x \gg 1$ then substituting $x = 2y$ into equation (25) indicates by comparison with equation (15) that the x axis intercept of the high q asymptote should equal that of the extrapolated low q intercept if the OAM applies. In *Figure 5*, calculated high q asymptotic gradients are shown assuming the interparticle scattering term is negligible for the two curves plotted. (Provided the interparticle term is q independent then it will, however, only affect the intercept of the extended Zimm plots and not their shapes or gradient.) The high q asymptote for $Kc/M_1 \geq 10$ was found to fall approximately on the low q data (see *Figure 5*). These results suggest that if the availability of data is restricted in the low u_z range then for concentrations where Kc/M_1 is large use of the Zimm expression over an extended q range could provide a better estimate of the weight average molecular weight and z-average radius of gyration for aggregating polymers that form Gaussian aggregates than fitting the Debye model for monodisperse Gaussian chains.

At high q, equation (25) simplifies further to give

$$[I(q)/\kappa cM_1]_{q\to\infty} \approx [2u_1^{-2}] \tag{28}$$

Figure 3 also indicates that as Kc/M_1 is raised the range over which equation (28) is valid (or double logarithmic and Kratky plots linear) increases. This range is expected to be reduced, however, if interparticle scattering effects become large (compare *Figure 1* and *Figure 3*). More generally for $k = 1$ and fractal objects it can be shown that providing A and D are independent of the number of chains in an aggregate then on combining equations (12) and (14)

$$[I(q)/\kappa cM_1]_{q\to\infty} \approx [Au_1^{-D}] \tag{29}$$

$k > 1$. If k is larger than 1, D for the aggregates is assumed equal to 2 and the Debye model is again used for both $S_1(q)$ and $S_n(q)$, then at $ku_1 > 1$ the double logarithmic curves of $I(q)/(\kappa cM_1)$ versus ku_1 do not merge (see for example *Figure 6* with $k = 2$). The asymptotic gradients, however, still all tend to a maximum value of 2. If k is only slightly larger than 1 it can be assumed as a first approximation that A and D in equation (12) are independent of the extent of aggregation as is the case for the curves in *Figure 6*. Then it can be shown that in general combining equation (22) and equation (23) with equation (12) and equation (14) gives

$$[I(q)q^D/(\kappa cM_1)]_{q\to\infty} \approx [A/Rg_{1,h}^D][w_1(k^D - 1) + 1] \tag{30}$$

D and $[I(q)q^D/(\kappa cM_1)]_{q\to\infty}$ can be obtained from Kratky plots at various concentrations. w_1 as shown by equation (18) and equation (19) is a function of Kc/M_1 only. Then plotting $[I(q)q^D/(\kappa cM_1)]_{q\to\infty}$ against w_1 provides a method of obtaining k and $Rg_{1,h}$ (provided A is known).

In *Figure 7* a normalized set of curves is given using $k = 2$, assuming D in equation (22) equals 2 for the aggregates, the hard sphere model [equation (3)] for $S_n(q)$ and the Debye expression for $S_n(q)$. In *Figure 8* the same set of conditions

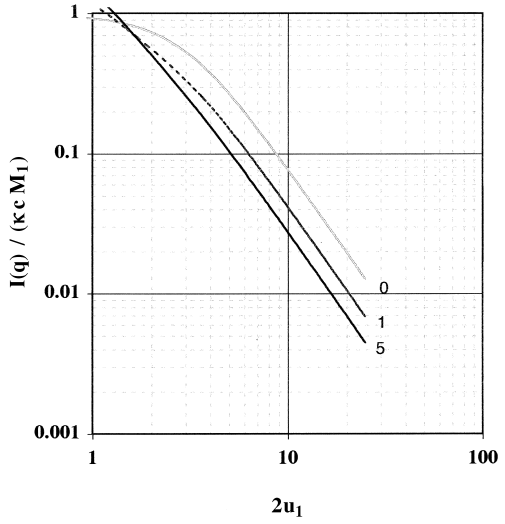

Figure 6 Calculated single chain molecular weight normalized scattering for a system aggregating via the open association model where the Debye model is used for $S_i(q)$ for both single chains and aggregates. In this example $D = 2$ and $k = 2$. Values for Kc/M_1 for each curve are given on the figure

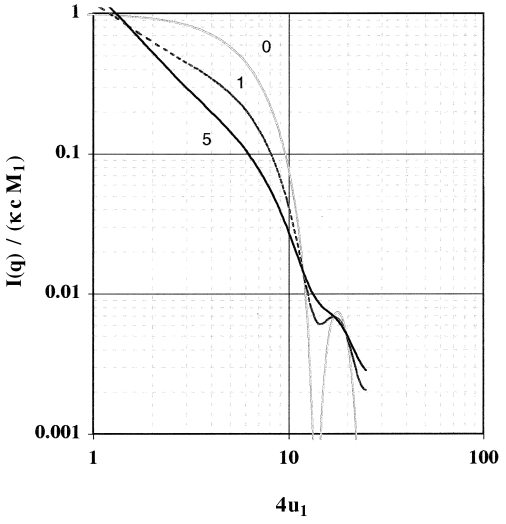

Figure 8 Single chain molecular weight normalized scattering for a system aggregating via the open association model where the Debye model is used for $S_n(q)$, the hard sphere model for $S_1(q)$. In this example $D = 2$ and $k = 4$. Values for Kc/M_1 for each curve are given on the figure

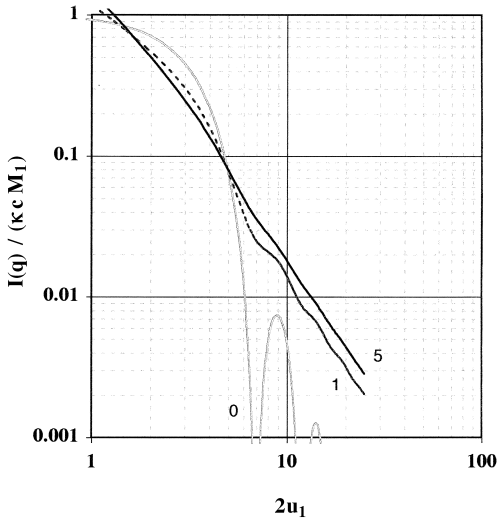

Figure 7 Calculated single chain molecular weight normalized scattering from a system aggregating via the open association model where the Debye model is used for $S_n(q)$, the hard sphere model for $S_1(q)$ $D = 2$ and $k = 2$. Values for Kc/M_1 for each curve are given on the figure

is used except that k is increased to a value of 4. In these examples for $u_z < k$ the scattering is dependent upon Rg_z and x only. *Figures 6–8* also indicate that at $u_z > k$ if all the scattering objects do not have the same fractal dimension then the scattering can be highly sensitive to Kc/M_1, q range, the magnitude of k and the model chosen for the single chains as well as the aggregates. The asymptotic high q gradient will not in these cases equal $-D$.

In summary the above results suggest that due to the large number of variables for systems aggregating via the OAM results should be obtained over as broad a concentration and q range as possible in order to confirm the validity of the model for the system. By the fitting of models to scattering data the equilibrium constant for the aggregation process, the size and shape of the single chains and aggregates and the magnitude of interparticle scattering effects might be obtainable. As a method of analysing the scattering from an aggregating system, as a first step Zimm plots can be used at low q to obtain average apparent molecular weights and radii of gyration. Care must be taken, however, to ensure that the range of q used is valid. From these the equilibrium constant and the radii of gyration of the single chains and aggregates can be estimated provided the effects of interparticle scattering are known or can be modelled.

Scattering at high q can readily be used via double logarithmic or Kratky plots to obtain the fractal dimension of the single chains and aggregates but only if the fractal dimension of all the scattering objects is the same and interparticle scattering effects are relatively small. If the fractal dimension of the aggregates and single chains are very different, however, then model curves need to be calculated and compared with data. Model curves are required to explain the scattering for an aggregating system in intermediate q ranges. The production of model curves of normalized intensity versus u_1 provides a convenient method of determining the effects of various parameters on the scattering from aggregating systems over a broad q range. These should be compared with data over a broad q range and at several concentrations simultaneously to ensure a reasonable single model fits all data available.

EXPERIMENTAL

Sample preparation

The sodium sulphonated polystyrene ionomer of molecular weight 105 000 and sulphonation level 1.39 mole % was prepared as described previously[24]. Briefly the procedure involves the random sulphonation of monodisperse (weight divided by number average molecular weight is less than 1.05) polystyrene in solution using acetyl sulphate. Solutions of the ionomer with concentrations between 0.5 and 6 g/dl were prepared by dissolving the required amounts of polymer in xylene d_{10} and sonicating the solutions in a water bath for 2 h. Even very dilute ionomer solutions can take a long time to reach equilibrium due to the very slow break up of aggregates that can be formed during the preparation of the ionomer. Sonication in a water bath visibly increases the initial rate of ionomer dissolution without causing, in this case, any measurable main chain scission. This has been confirmed in earlier

studies[25]. Other methods used during the ionomer preparation that help reduce the time required for equilibrium to be obtained have been reported and interpreted in detail previously[24,25]. All the ionomer solutions and gels were prepared one month before SANS measurements were performed. Over this period of time the more concentrated solutions (> 2.5 g/dl) changed from low viscosity solutions to gel-like fluids that flow only very slowly on inverting the container. Examples of the viscosity versus time in gelling ionomer solutions and some preliminary static light scattering studies on these gels are given in earlier work[24,25]. The latter results indicate that at $q < 0.05$ Å^{-1} the intensity of scattering from the gels decreases with time for many weeks after the initial solution preparations. This is believed to be as a result of scattering from a few very large aggregates that fail to be properly dispersed. At higher q, however, these very large aggregates have little effect on the scattered intensities and no further change with time in the scattering is observed for these ionomer gels at $q > 0.05$ Å^{-1} after about 8 days.

Small angle neutron scattering

Small angle neutron scattering experiments were performed using the LOQ spectrometer at the Rutherford Appleton laboratory. The LOQ instrument at the ISIS pulsed neutron source records the time of flight of neutrons of wavelengths 2.2 to 10 Å onto a 64 cm square position-sensitive ^{3}He detector at 4.05 m from the sample. Time of flight and position are converted to neutron wavelength and scattering angle. The raw data are corrected for the wavelength dependence of the incident spectrum, detector efficiencies and sample transmission in order to generate a scattering cross-section, in absolute units, for a wavevector range of 0.009–0.24 Å^{-1}. The more dilute solutions were measured in 2 mm path length quark cells at 25°C. The gelled samples were placed between two quartz plates separated by a spacer of 2 mm.

Model fitting

In the following procedures all observed intensities were first normalized by κ, c and M_1 using a spreadsheet program. In most cases the latter constants were fixed at the known values in order to reduce the number of variables in the data fitting procedures. Fitting of linear expressions [for example equation (15) to determine M_{app} and Rg_{app}] or quadratic equations (to gain $\langle M \rangle_w$, A_2 and A_3 for polystyrene) was carried out using Cricket Graph 1.2b™. For more complex expressions variables were determined by comparing calculations with data. Examples include estimation for the ionomer of K, A_2 and A_3 [calculations require equations (9) and (18)] from M_{app} versus concentration or Rg_1, $Rg_{1,h}$ and D for the aggregates from calculated values of Rg_z x versus concentration. In the calculation of Rg_z [using equations (18)–(22)] or model scattering curves typically aggregates consisting of up to 50 chains were considered. Larger aggregates have negligible effect on the scattering provided $Kc/M_1 < 10$. All such calculations were carried out using spreadsheets.

With the normalized scattering intensities versus q in double logarithmic form, results can be conveniently overlaid on model curves simply by shifting data plots horizontally. This is provided the numbers of decades per unit length on the axes are equal for both the data and model curves. As well in the following study the data and model curves were plotted on the same figure using the spreadsheet program. Comparison of figures such as *Figures 1–8* with actual data was achieved by multiplying q values for the data by a single variable (equal to either Rg_1, Rg_z or kRg_1) until good agreement between the normalized intensities and that predicted by a model was obtained.

RESULTS

In the following the scattering from polystyrene in xylene will first be briefly discussed. This is aimed initially at giving some confidence in the data normalization and also provide confidence in the methods used to interpret the scattering data since the behaviour of polystyrene in similar solvents is well understood. The effect on the scattering after adding just a few ionic groups to the polymer to produce an ionomer in the same solvent will then be described. Such a comparison from two polymers (PS and SPS) that are chemically almost identical (since there are only what might be considered impurity levels of ionic groups in the ionomer) will also provide a good comparison of the scattering from aggregating and non-aggregating polymers.

Polystyrene in xylene

In *Figure 9* examples of concentration and molecular weight normalized scattering from polystyrene in xylene is

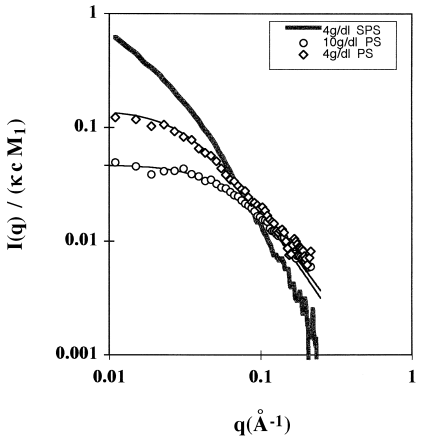

Figure 9 Normalized scattering from polystyrene and SPS in xylene. Lines through the polystyrene data are the best fits of the Zimm expression (equation (1)) with the Debye model for $S(q)$ (equation (4))

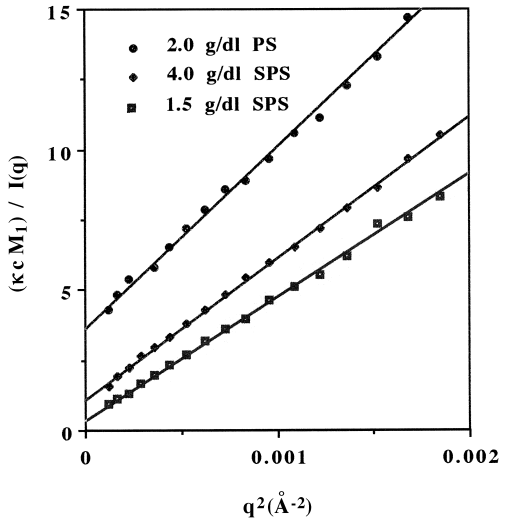

Figure 10 Examples of low q Zimm plots for polystyrene and SPS in xylene

Table 1 Apparent molecular weights and radii of gyration for polystyrene in xylene at 25°C

Concentration c (g/dl)	Parameters from				
	Low q Zimm analysis[a]			Debye analysis[b]	
	M_{app}/M_1[c]	Rg_{app} (Å)	Rg_z (Corrected)[d] (Å)	Rg_z (Å)	$2A_{2,app}M_1c$
2.0	0.281	74	140 (116)	110 (± 5)	3
4.0	0.142	47	125 (104)	100 (± 5)	6
6.0	0.094	36	117 (98)	95 (± 5)	10
10.0	0.047	23	107 (89)	90 (± 5)	20

[a]Results obtained using equation (6) with data in the range $1 < qRg_z < 4$.
[b]Results obtained by fitting equation (1) with equation (4) and equation (11) over the range $1 < qRg_z < 4$.
[c]Since the polystyrene sample is monodisperse $< M >_w = M_1$.
[d]Radii of gyration have been corrected for the use of too high a q range by dividing actual values obtained from Zimm plots by the factor 1.2.

shown. In the limit of zero concentration and q this normalized intensity should tend to a value of 1 for a non-aggregating polymer. The intensity decreases at low q, however, as the polymer concentration is raised. This is due to the effects of interparticle scattering.

Zimm analysis of polystyrene scattering. In *Figure 10* a Zimm plot for a polystyrene solution at 2 g/dl is given. Unfortunately there is insufficient accurate data in the low q range due to the low scattering intensities to detect curvature of the plot as would be expected if the Debye model is valid (see *Figure 5*). M_{app} and Rg_{app} [defined by equations (9) and (10)] obtained from such Zimm plots using data in the range $0.0001 < q^2(\text{Å}^{-2}) < 0.002$ are shown in *Table 1*. Fitting of a polynomial of order 2 to $1/M_{app}$ versus concentration gave using equation (9) $\langle M \rangle_w = 82\,000$ g mol^{-1}, $A_2 = 4.6 \times 10^{-4}$ mol g^{-2} cm^3 and $A_3 = 3.2 \times 10^{-3}$ mol g^{-3} cm^6. The first two parameters ($\langle M \rangle_w$ and A_2) are, however, in reasonable agreement with results obtained previously using light scattering[25] despite the use of data outside the range $qRg < 1$ and low accuracy of the data. Z-average radii of gyration calculated from the apparent values [using equation (10)] are also given in *Table 1*. Z-average radii of gyration for polystyrene of 10^5 g mol^{-1} in aromatic solvents have been obtained previously using the neutron contrast match variation method. The latter technique uses a mixture of hydrogenous and deuterated polymer in mixed hydrogenous and deuterated solvents and provides a more direct method of separating interparticle from intraparticle scattering. In toluene Rg decreasing from 120 to 105 Å between 2 and 10 g/dl[22] and in xylene Rg equal to 105 Å at 3 g/dl[24] were observed. Comparison of the polystyrene dimensions in this study with previous work suggests that use of the Zimm expression in the above q range results in radii of gyration that are about 20% too large. Ullman[26], however, has provided correction factors for radii of gyration obtained using too broad a range of q. After use of these correction factors the radii of gyration obtained in this work become comparable with previous studies (see *Table 1*).

Kratky plots for polystyrene. At 2 g/dl both Kratky plots and log I versus log q at high q indicated that D is 1.6 ± 0.1 for polystyrene in xylene, which is in agreement with theoretical expectations[21]. Kratky plots for the other higher concentration polystyrene solutions, however, did not become horizontal in the high q range when realistic values for D (between 1.5 and 2) were used. This arises because the interparticle scattering term, $2A_{2,app}M_1c$, is not negligibly small in comparison with $u_1^2/2$ until $q > 0.1$ Å^{-1}.

Model fitting of polystyrene data. Alternatively the polystyrene data can be compared with curves such as those in *Figure 1*, which were calculated using equations (1) and (4). Estimates of the interparticle effect, $2A_{2,app}M_1c$, and Rg_1 obtained by this method as a function of concentration are given in *Table 1*. Examples of fits are shown with the polystyrene data in *Figure 9*. From the concentration dependence of $2A_{2,app}M_1c$ using equation (11) $A_2 = 6.2 \times 10^{-4}$ mol g^{-2} cm^3 and $A_3 = 2.1 \times 10^{-3}$ mol g^{-3} cm^6 are obtained. Both the virial coefficients and the radii of gyration (see *Table 1*) are in reasonable agreement with the values determined by the Zimm plot method described above considering that in this case M_1 was fixed at 105 000 g mol^{-1}.

Summary of polystyrene behaviour. It should be noted that for the polystyrene sample in this study the theta radius of gyration is 93 Å[14]. The polystyrene molecules in xylene are therefore expanded in dilute solution but decrease to the theta dimensions at about 10 g/dl. The similarity between all the various parameters determined by the two different methods of analysis described above suggest that although the Debye model has been designed for unperturbed polymers, it also provides [when combined with equation (1)] a reasonable estimate of the scattering from slightly expanded polystyrene in aromatic solvents over quite a broad q range. Developed but similar methods for interpreting the scattering from aggregating ionomers also in xylene will be described in the following.

Sulphonated polystyrene in xylene

At low q the scattering from an ionomer solution or gel is very much more intense than from an equivalent polystyrene solution (see *Figure 9*). In *Figure 11* examples of scattering from an ionomer solution and gel are shown. At the ionomer gelation threshold concentration of 2 g/dl there is no abrupt change in the shape or intensity of scattering curves. As with polystyrene solutions, however, the concentration and molecular weight normalized ionomer solution scattering between 1.5 and 6 g/dl in the low q range decreases steadily as the ionomer concentration is raised presumably as a result of increasing intermolecular scattering effects. The latter is contrary to what is observed in the more dilute ionomer solutions where an increase in normalized scattering at low q occurs on raising the ionomer concentration due to increasing extent of aggregation.

Zimm analysis of ionomer data. Examples of normalized inverse intensities plotted against q^2 for an ionomer solution and gel are shown in *Figure 10*. As observed for polystyrene in xylene no significant curvature of these

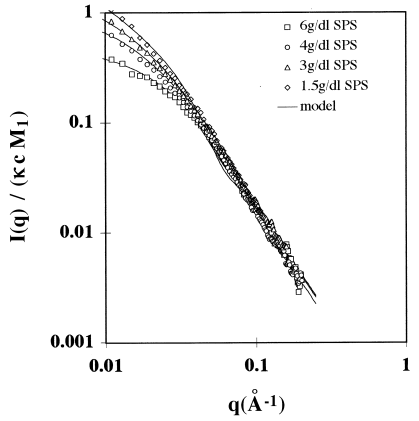

Figure 11 Examples of normalized scattering from SPS in xylene. Lines through the data are the calculated curves determined using equation (14) as described in the text

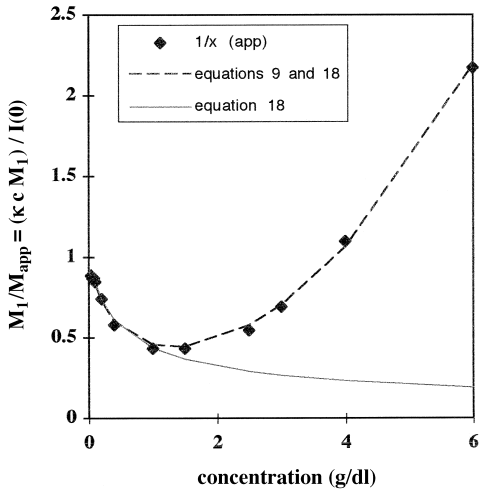

Figure 12 Apparent inverse molecular weights as a function of concentration for SPS in xylene. The lines are the best fit of equation (18) (using data below 1 g/dl only) or equation (18) with equation (9) over the full concentration range

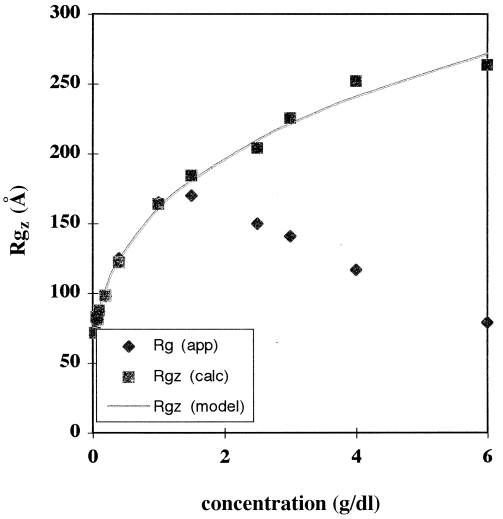

Figure 13 Apparent and calculated *z*-average radii of gyration for SPS in xylene. The model curve is the best fit of equation (21)

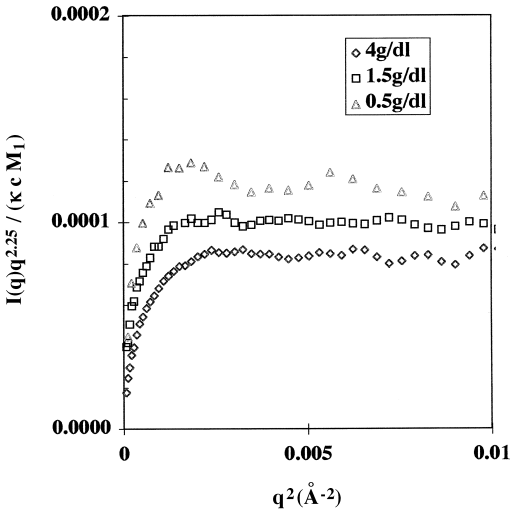

Figure 14 Examples of Kratky plots for SPS in xylene

Zimm plots is observed in the range $0.0001 < q^2\,\text{Å}^{-2} < 0.002$. Inverse apparent molecular weights estimated from the extrapolated zero q intercepts from both previous dilute solution work[11] and semi-dilute solutions (this study) are plotted as a function of concentration in *Figure 12*. A good fit of the OAM [assuming equations (9) and (18) are valid] for the ionomer solutions and gels over the whole concentration range measured could be obtained using $K = 0.105\ \text{cm}^3\,\text{mol}^{-1}$, $A_2 = -0.2 \times 10^{-4}\ \text{mol g}^{-2}\,\text{cm}^3$ and $A_3 = 19.8 \times 10^{-4}\ \text{mol g}^{-3}\,\text{cm}^6$ (see *Figure 12*). Calculated inverse weight average molecular weights [using equation (18)] are also given in this figure. The similarity between calculated and apparent values of x only below 1 g/dl indicates that interparticle scattering effects are negligible only below this concentration. The good fit of the model curve to all the results suggests that even when the ionomer solutions appear to gel the extent of aggregation of the ionomers chains can still be predicted by the OAM. (N.B. Rather conveniently $K/M_1 = 1.0$ dl/g so Kc/M_1 values in earlier figures can be taken as equivalent to c in g/dl for the ionomer solutions.)

Apparent radii of gyration obtained for the ionomer using the Zimm plots are plotted against concentration in *Figure 13*. *Z*-average radii of gyration for the ionomer calculated from the Zimm apparent values [using the virial coefficients calculated above and equation (10)] are also given in *Figure 13*. The best fit of equation (21) [using $K/M_1 = 1.0$ dl/g and equations (18) and (22)] to the z average radii of gyration was observed with $Rg_1 = 60 \pm 5$ Å, $Rg_{1,h} = 85 \pm 5$ Å and $D = 1.7 \pm 0.2$ (see *Figure 13*).

Kratky type analysis of ionomer data. Unlike most of the polystyrene data Kratky plots for all the ionomer solutions did exhibit a horizontal plateau range between $0.05 < q\text{Å}^{-1} < 0.1$ (see *Figure 14*). The difference between the two polymers is likely to arise because of the effects of aggregation combined with the reduced interparticle scattering for the ionomer. Using the virial coefficients determined above [with equation (11)] at the highest ionomer concentration investigated of 6 g/dl the interparticle term $2A_{2,\text{app}}M_1c$ equals 10 for polystyrene but only 1.0 for the ionomer. The values of D obtained from Kratky plots for the ionomer were found to be within experimental error practically independent of concentration between 1.0 and 6 g/dl and equal to 2.25 ± 0.05 if data between the above limits were used.

Since the value of D did not vary significantly with concentration $[I(q)q^{2.25}/(\kappa cM_1)]_{q\to\infty}$ was plotted against w_1 [see equation (30) and *Figure 15*]. From the gradient of this plot $k = 1.4 \pm 0.2$. Assuming A = 2, as required for

Gaussian coils (a reasonable first aproximation since D is close to 2), $Rg_{1,h} = 91 \pm 5$ Å is obtained from the intercept. From equation (23) this then gives $Rg_1 = 65$ Å. Both the latter dimensions are within experimental error in agreement with those obtained from the lower q data. The magnitude of D, however, is significantly larger than obtained above. This is likely to be a consequence of the observed value of D being assumed to be equal for both the single chains and aggregates in the Kratky method of analysis. The presence, particularly in the gels, of a few large aggregates that are not properly dispersed to an equilibrium state could also in part cause discrepancy between interpretation of low and higher q data. These aggregates would be expected to have much larger effects on the values obtained for Rg_z than on high q scattering.

Model fitting high q ionomer data. When the scattering from the ionomer solutions is compared with the previously calculated model curves *Figure 7* provided the best description of the concentration dependence of the scattering behaviour for $q > 0.05$ Å^{-1} of all the figures shown. (In this range interparticle scattering effects can be assumed negligible for all the ionomer solutions and gels investigated.) *Figure 7* uses the hard sphere model for the single chains and the Debye model for the aggregates. The other calculated models either predicted an insufficiently steep gradient (see examples in *Figures 3, and 6*) or too large a concentration dependence of the high q scattering (compare *Figure 11* with *Figures 6* and *8*). Using the hard sphere model for the single chains and the Debye model for the aggregates similar curves to those given in *Figure 7* were produced for various values of D for the aggregates and k. In all cases with k values between 1 and 2 the calculated dependence of scattering at $q > 0.05$ Å^{-1} was found to have only minor sensitivity to the magnitude of K/M_1 or D for $Kc/M_1 > 1$. Comparison of ionomer data with a range of curves of varying k, however, could provide an estimate of k and $Rg_{1,h}$. Assuming $K/M_1 = 1.0$ dl/g and $D = 2k = 1.75 \pm 0.25$ and $Rg_{1,h} = 95 \pm 5$ Å were obtained. These results give Rg_1 equal to 54 Å.

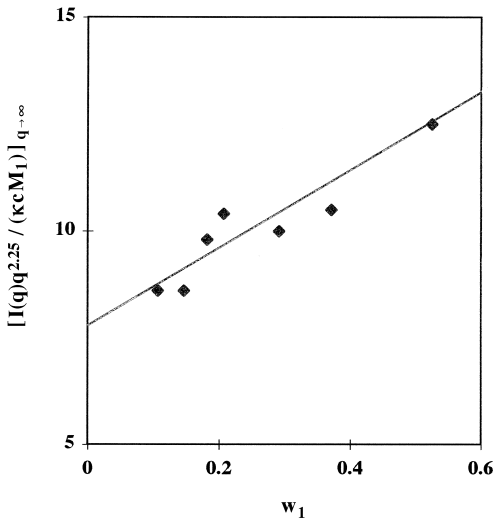

Figure 15 $[I(q)\, q^{2.25}/(\kappa c M_1)]_{q\to\infty}$ versus weight fraction of single chains for SPS in xylene

Summary of ionomer scattering behaviour. All the parameters obtained above by the various methods are summarized and given with averaged values in *Table 2*. Using these averaged values, the hard sphere model for the single chains and the Debye expression for the aggregates, model curves were calculated [using equation (14)] for the full q range investigated. These model curves are compared with data for the ionomer in *Figure 11*. At all concentrations the model curves fit the data well within the experimental error limits over the whole q range measured.

DISCUSSION

Since xylene is a poor solvent for the ionic groups but a good solvent for polystyrene, A_2, as observed above, might be expected to be smaller for the ionomer than for the base polystyrene. The value of the third virial coefficient for the ionomer lies between that observed for polystyrene in xylene and in theta solvents at the theta temperature[27]. The small negative second virial coefficient for the ionomer is consistent with the observation that if the sulphonation level for a gelling ionomer solution is raised slightly the ionomers become insoluble[1]. An alternative method of interpreting interparticle scattering would be to consider the interaction potentials between two of the aggregates[21]. The very small value of A_2 suggests that attractive interactions between the polymer aggregates just balance the repulsive interactions.

Rg_1 obtained in this work has an identical value to that previously obtained using contrast matched SANS at low concentrations for a very similar ionomer in xylene[24]. Its value is smaller than that expected for polystyrene in a theta solvent of 93 Å, which gives further evidence that the second virial coefficient should be negative. A hard sphere of polystyrene with a density $\rho = 1$ g/dl from the equation for the volume of a sphere ($V = M_1/N_a\rho = 4/3\ \pi R^3$) would be expected to have a radius, R, of approximately 35 Å (equivalent to Rg equal to only 27 Å). Given the value used in our fit ($Rg_1 = 60$ Å) this suggests that the hard sphere model does not give a perfect description of the single chain structure. A better description for the single chains might be starlike or a core/shell type structure. Attempts were made to model the single chains as Gaussian stars. It was found, however, that much more accurate results at considerably lower concentrations would be required to assess whether alternative models would better describe the scattering from the compact ionomer single chains over a broad q range.

Between 1 and 6 g/dl using $K/M_1 = 1.0$ dl g^{-1} from *Figure 1* most of the ionomer aggregates will consist of

Table 2 Summary of parameters obtained from fitting ionomer data

Method of analysis	qRg_1 range used	$10^{-8}K$ (cm^3 mol^{-1})	10^4 A_2 (mol g^{-2} cm^3)	10^4 A_3 (mol g^{-3} cm^6)	Rg_1 (Å)	$Rg_{1,h}$ (Å)	D
Zimm plots	0.6–3	0.105 ± 0.005	−0.2 ± 0.2	19.8 ± 0.5	60 ± 5	85 ± 5	1.7 ± 0.2
Kratky plots	4–15	0.105[a]	–	–	65 ± 5	91 ± 5	2.25 ± 0.05
Model fitting	4–15	0.105[a]	–	–	54 ± 5	95 ± 5	2[a]
Average	0.6–15	0.105	−0.2	19.8	60	90	2

[a]These parameters were fixed in the analysis.

between 2 and 5 chains. The dimensions of these aggregates calculated using $R_{1,h}$ and D [with equation (22)] are compared with values expected for Gaussian polystyrene coils, solid spheres and polystyrene in xylene in *Figure 16*. From this figure it can be seen that the aggregate dimensions are close to those observed for unperturbed polystyrene. This is consistent with the Debye model, describing well the scattering from the ionomer aggregates.

From previous X-ray scattering studies it has been shown for similar ionomer/solvent systems that within an aggregate the ion pairs associate into clusters consisting of up to about 10 sulphonate groups[28]. Other SANS studies also indicate that within the aggregates the individual ionomer chains can expand. It has been proposed that driving force for the aggregation is the increased configurational entropy of the polymer combined with free energy changes associated with the greater ability of the polystyrene to mix with the solvent when the ionomer forms more expanded aggregates[13]. The open association model assumes that the total increase in free energy each time a single chain joins an aggregate is independent of the aggregate size[15]. An improvement in the model could be made by allowing this free energy to vary with aggregate size. It is felt, however, that the results for the ionomer in this study do not deviate sufficiently from the simple open association model to make it necersary to increase the number of variables. A schematic two-dimensional final summary diagram representing the single chains and two chain aggregates that takes into account all the above known information on the aggregate structures and single chain dimensions is given in *Figure 17*.

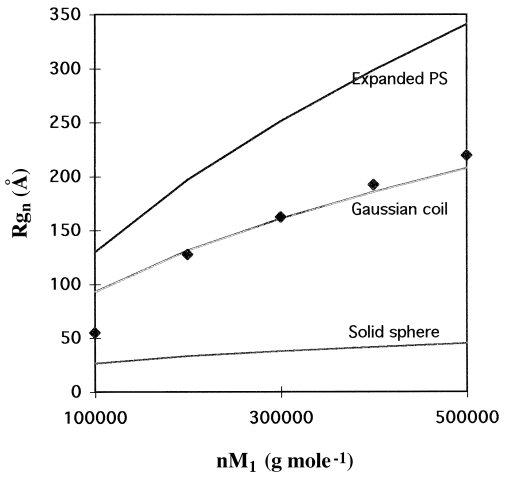

Figure 16 Aggregate and single chain radii of gyration versus molecular weight (Zimm-type analysis results). Lines are the expected values for solid spheres or Gaussian coils of polystyrene and the dimensions of polystyrene in xylene at the aggregate molecular weights

Semi-dilute solutions of very high molecular weight polymers in theta solvents can show similar rheological features to the above ionomer gels[24,29]. Although most of the aggregates within the above ionomer solutions and gels are fairly small the OAM does predict the presence of increasing levels of very large aggregates once the gelation concentration is reached. These results suggest that it is interactions between these large aggregates combined with the practically zero free energy of mixing polymer and solvent (indicated by the small virial terms) that account for the ionomer solutions' gelation.

CONCLUSIONS

Several methods have been used above to interpret both the low and high q scattering from ionomer solutions and gels. All the results are consistent with the open association model interpreting the extent of aggregation of the ionomers with concentration both within the dilute solutions and the gels. Isolated single chains are found to be very compact at all concentrations whereas the dimensions of the aggregates are comparable with those of unperturbed polystyrene of the aggregate molecular weight. When the ionomer gelation threshold concentration is approached there is no abrupt change in the structure or size of the aggregates but just a gradual increase in the numbers of very large aggregates. Further work on other systems is required to ascertain what are the relationships between the gelation threshold concentration, the aggregate dimensions or aggregation equilibrium constant and the possible importance of the free energy of mixing the ionomer and solvent.

In general this work has shown that interpretation of the scattering from gelling solutions can be complex due to a combination of increasing aggregation of the polymer chains with concentration, inter-aggregate scattering effects and non-fractal nature of the single chains and aggregates. The modelling methods developed in this study need to be extended and applied to other systems such as telechelic ionomers in order to confirm whether the open association

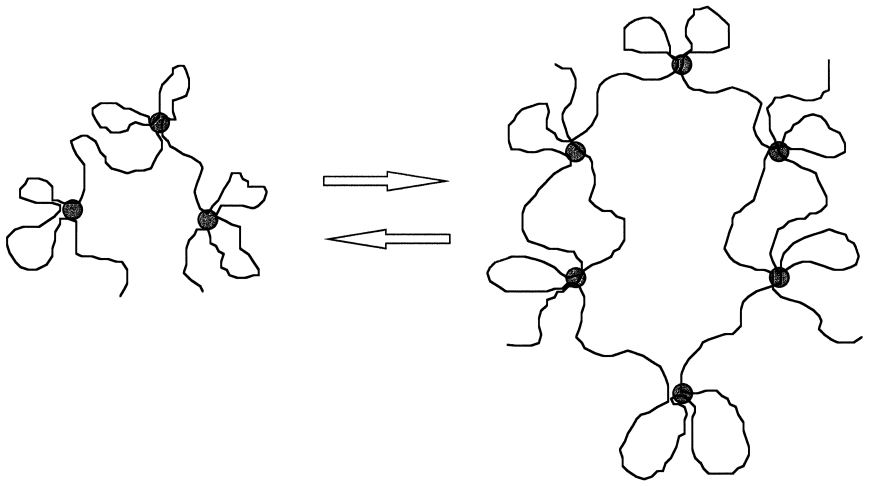

Figure 17 Schematic two-dimensional representation of the ionomer single chains and two chain aggregates. Circles represent clusters of three ion pairs

model can interpret the scattering from other solutions that are capable of gelling. This type of modelling might also help in the interpretation of the scattering under shear from shear thickening ionomer solutions that has previously been difficult to quantitatively explain[25].

REFERENCES

1. Agarwal, P. K., Garner, R. T. and Graessley, W. W., *J. Polym. Sci. Polym. Phys. Edn.*, 1987, **25**, 2095.
2. Tant, M. R. and Wilkes, G. L., *JMS-REV. Macromol. Chem. Phys.*, 1988, **C28**, 1.
3. Chakrabarty, K., Shao, P. and Weiss R. A., in *Ionomers: Synthesis, Structure, Properties and Applications*, ed. M. R. Tant, K. A. Mauritz and G. L. Wilkes, Blackie Academic, London and New York, 1997, pp. 158–207.
4. Lundberg, R. D., in *Structure and Properties of Ionomers*, ed. M. Pineri and A. D. Eisenberg. Reidel, Dordrecht, 1987, pp. 429–438.
5. Lundberg, R. D., in *Ionomers: Synthesis, Structure, Properties and Applications*, ed. M. R. Tant, K. A. Mauritz and G. L. Wilkes, Blackie Academic, London and New York, 1997, pp. 477–501.
6. Pezron, I., Djabourov, M. and Leblond, J., *Polymer*, 1991, **32**, 3201.
7. Cogrove, T., White, S. J., Zarblakash, A., Heenan, R. K. and Howe, A. M., *J. Chem. Soc. Faraday Trans.*, 1996, **92**, 595.
8. Kobayashi, M., Yoshioka, T., Imai, M. and Itoh, Y., *Macromolecules*, 1995, **28**, 7376.
9. Kanaya, T., Ohkura, M., Takeshita, H., Kaji, K., Furusada, M., Yamaoka, H. and Wignal, G. D., *Macromolecules*, 1995, **28**, 3168.
10. Pedley, A. M., Higgins, J. S., Peiffer, D. G. and Burchard, W., *Macromolecules*, 1990, **23**, 1434.
11. Young, A. M., Higgins, J. S., Peiffer, D. G. and Rennie, A. R., *Polymer*, 1995, **36**, 691.
12. Young, A. M., Timbo, A. M., Higgins, J. S., Peiffer, D. G. and Lin, M. Y., *Polymer*, 1996, **37**, 2701.
13. Young, A. M., Higgins, J. S., Peiffer, D. G. and Rennie, A. R., *Polymer*, 1996, **37**, 2125.
14. Young, A. M., Garcia, R.,Timbo, A. M., Higgins, J. S. and Peiffer, D. G., *Polymer*, 1998, **39**, 1525.
15. Elias, H. G., in *Light Scattering from Polymer Solutions*, ed. M. B. Huglin. Academic Press, London, 1972, Chapter 9.
16. Timbo, A. M., Higgins, J. S., Peiffer, D. G., Maus, C., Vanhoorne, P. and Jerome, R., *Journal De Physique IV*, 1993, **3**, 71.
17. Karayianni, E., Jerome, R. and Cooper, S. L., *Macromolecules*, 1995, **28**, 6494.
18. de Gennes, P. G., *Scaling Concepts in Polymer Physics*. Cornell University, Ithaca, NY, 1979.
19. Boue, F., Nierlich, M. and Leibler, L., *Polymer*, 1982, **23**, 29.
20. Glatter, O. and Kratky, O., *Small Angle X-ray Scattering*. Academic Press, London, 1982.
21. Higgins, J. S. and Benoit, H. C., *Polymers and Neutron Scattering*. Oxford University Press, Oxford, 1994.
22. King, J. S., Boyer, W., Wignal, G. D. and Ullman, R., *Macromolecules*, 1985, **18**, 709.
23. Ullman, R., Benoit, H. and King, J. S., *Macromolecules*, 1986, **19**, 183.
24. Pedley, A. M., Higgins, J. S., Peiffer, D. G., Rennie, A. R. and Staples, E., *Polymer Communications*, 1989, **30**, 162.
25. Pedley, A. M., Ph.D. Thesis, Imperial College, 1990.
26. Ullman, R., *J. Polym. Sci. Polym. Phys. Ed.*, 1985, **23**, 1477.
27. Kinugas, S., Hayashi, H., Hamada, F. and Nakajima, A., *Macromolecules*, 1986, **19**, 2832.
28. Vanhoorne, P. and Jerome, R., in *Ionomers Characterisation, Theory, and Applications*, Chap. 9, ed. S. Schlick. CRC Press, New York, 1996.
29. Bradna, P. and Quadnat, O., *Colloid Polym. Sci.*, 1984, **262**, 189.